Unified Formulation of the Aeroelasticity of Swept Lifting Surfaces

PIERGIOVANNI MARZOCCA*, LIVIU LIBRESCU*†

and

WALTER A. SILVA‡

* Engineering Science and Mechanics Department, Virginia Polytechnic Institute and State University, Blacksburg, VA 24061-0219, USA.

and

‡ NASA Langley Research Center, Hampton, VA 23681-2199, USA.

† Corresponding author

Office: (540) 231 – 5916 Home: (540) 953 – 0499

Fax: (540) 231 – 4574 Email: librescu@vt.edu

Running Title: **Unified Formulation of the Aeroelasticity of Swept Lifting Surfaces**

Unified Formulation of the Aeroelasticity of Swept Lifting Surfaces

Piergiovanni Marzocca* and Liviu Librescu†

Virginia Polytechnic Institute and State University, Blacksburg, VA 24061-0219,

and

Walter A. Silva‡

NASA Langley Research Center, Hampton, VA 23681-2199.

Abstract

An unified approach for dealing with stability and aeroelastic response to time-dependent pressure pulses of swept wings in an incompressible flow is developed. To this end the indicial function concept in time and frequency domains, enabling one to derive the proper unsteady aerodynamic loads is used. Results regarding stability in the frequency and time domains, and subcritical aeroelastic response to arbitrary time-dependent external excitation obtained via the direct use of the unsteady aerodynamic derivatives for 3-D wings are supplied. Closed form expressions for unsteady aerodynamic derivatives using this unified approach have been derived and used to illustrate their application to flutter and aeroelastic response to blast and sonic-boom signatures. In this context, an original representation of the aeroelastic response in the phase – space was presented and pertinent conclusions on the implications of some basic parameters have been outlined.

* Aerospace Engineer, Ph.D. Student.
† Professor of Aeronautical and Mechanical Engineering, Department of Engineering Science and Mechanics.
‡ Senior Research Scientist, Senior Aerospace Engineer, Aeroelasticity Branch, Structures Division, Senior Member AIAA.

Nomenclature

a_n Dimensionless elastic axis position measured from the midchord, positive aft

c_n Chord length of wing, normal to the elastic axis, $2b_n$

$C_{L\alpha_n}$ Lift-curve slope

$C(k), F(k), G(k)$ Theodorsen's function and its real and imaginary counterparts, respectively

f_h, f_α Plunging and pitching deflection functions

h, h_0 Plunging displacement and its amplitude, respectively

H_i, A_i Dimensionless unsteady aerodynamic coefficients

L_i, M_i Dimensionless unsteady aerodynamic complex coefficients

i Imaginary unit, $\sqrt{-1}$

I_y, $\bar{r}_\alpha$ Mass moment of inertia per unit length of wing and the dimensionless radius of gyration, $\left(I_y/mb_n^2\right)^{1/2}$, respectively

l Wing semi-span measured along the mid-chord line

l_h Dimensionless aerodynamic lift, $L_a b_n/mU_n^2$

$_\Lambda L_a, _\Lambda M_a$ Total lift and moment about the elastic axis per unit span of the swept wing

L_b, l_b Overpressure signature of the N-wave shock pulse and its dimensionless counterpart, $L_b b_n/mU_n^2$, respectively

m, μ Wing mass per unit length and wing/air mass ratio, $m/\pi\rho b_n^2$, respectively

m_a Dimensionless aerodynamic moment, $M_a b_n^2/I_y U_n^2$

N Load Factor, $1+h''/g$

$P_m, \wp_m$ Peak reflected pressure in excess and its dimensionless value $P_m b_n/mU_n^2$, respectively

r Shock pulse length factor

$s, \mathcal{L}$ Laplace transform variable and operator, respectively

$S_\alpha, \bar{\chi}_\alpha$ Static unbalance about the elastic axis and its dimensionless counterpart, S_y/mb_n, respectively

t, τ_0, τ Time variables and dimensionless time, $U_n t/b_n$, respectively

U_∞, U_n Freestream speed and its component normal to the elastic axis, respectively

V_n Dimensionless free-stream speed, $U_n/b_n\omega_\alpha$

x Coordinate parallel to freestream direction

$\bar{x}$ Chordwise coordinate normal to the elastic axis

y Coordinate perpendicular in the freestreem direction

$\bar{y}$ Spanwise coordinate along the elastic axis

w Downwash velocity

z Transverse normal coordinate to the midplane of the wing

Z Vertical displacement in z direction

α, α_0 Twist angle about the pitch axis and its amplitude, respectively

δ_r Tracer quantity

ζ_h, ζ_α Structural damping ratio in plunging, $c_h/2m\omega_h$ and in pitching, $c_\alpha/2I_y\omega_\alpha$, respectively

η Dimensionless coordinate along the wing span, $\bar{y}/l$

λ, σ Spanwise rate of change of twist and bending, respectively

Λ Swept angle (positive for swept back)

ξ Dimensionless plunge coordinate, w/b_n

ρ Air density

τ_p Dimensionless positive phase duration of the pulse, measured from the time of the arrival

$\phi(\tau), \Phi(s)$ Wagner's function in the time and Laplace domains, respectively

ω, k_n Circular and reduced frequencies, $\omega b_n / U_n$, respectively

ω_h, ω_α Uncoupled frequency in plunging, $(K_h/m)^{1/2}$ and pitching, $(K_\alpha / I_y)^{1/2}$, respectively

$\overline{\omega}$ Plunging-pitching frequency ratio, ω_h/ω_α

Subscript

$(\cdot)_c$ Circulatory terms of lift and aerodynamic moment

$(\cdot)_{nc}$ Non-circulatory terms of lift and aerodynamic moment

$(\cdot)_n$ Quantity normal to the elastic axis

${}_\Lambda(\cdot)$ Quantity associated with the swept wing

Superscript

$\hat{(\cdot)}$ Variables in Laplace transformed space

$\dot{(\cdot)}, (\cdot)'$ Derivatives with respect to the time t, and the dimensionless time τ, respectively

1. Introduction

In this paper, the concept of the linear indicial[1-3] functions in the time and frequency domains is used to determine the associated unsteady aerodynamic derivatives for swept lifting surfaces. Such a treatment of the problem enables one to approach either the open/closed loop aeroelastic response in the subcritical flight speed regime to arbitrary time-dependent external excitations (such as e.g. gusts, airblasts due to explosions or sonic-booms[4-5]), or the flutter instability of actively controlled/uncontrolled swept wings. In this paper both problems are addressed.

As by-product of this analysis, a close form solution of the unsteady aerodynamic coefficients is obtained that is directly used in the stability and aeroelastic response problems.

The unsteady aerodynamic lift and moment in incompressible flight speed regime are expressed for the swept aircraft wing in the time and frequency domains by using the Wagner and Theodorsen functions, respectively. For the response of dynamic systems it is only necessary to express the lift and moment via the indicial Wagner's function. For the approach of the flutter problem, the Theodorsen's function helps the conversion of the expressions of both the aerodynamic loads and the unsteady aerodynamic derivatives in the frequency domain[6-7].

Herein the case of a 3-D lifting surface, including the plunging and pitching degrees of freedom is considered for flutter and response analyses.

2. Preliminaries

As shown in Ref. 8, for zero initial conditions, the unsteady aerodynamic loads can be converted from the time to the frequency domain via a Laplace transform. This results in the possibility of using the correspondence $s \to ik_n$ as to convert the unsteady aerodynamic load from the time to the frequency domain, where s and k_n are the Laplace variable and the reduced frequency, respectively. The Laplace transform operator $\mathcal{L}$ is defined as:

$$\mathcal{L}(\cdot) = \int_0^\infty (\cdot) e^{-s\tau} d\tau . \tag{1}$$

In this sense, the Wagner's function $\phi(\tau)$ is connected with the Theodorsen's function $C(k_n)$ via a Laplace transform as:

$$\frac{C(k_n)}{ik_n} = \frac{F(k_n) + iG(k_n)}{ik_n} = \int_0^\infty \phi(\tau) e^{-ik_n\tau} d\tau = \Phi(ik_n), \tag{2}$$

and vice-versa:

$$\phi(\tau) = \mathcal{L}^{-1}\left\{C(k_n)/ik_n\right\}, \qquad Re(ik_n) > 0 . \tag{3}$$

and having in view the correspondence $s \leftrightarrow ik_n$ we can also write:

$$\Phi(ik_n) \underset{ik_n \to s}{=} \int_0^\infty \phi(\tau) e^{-s\tau} d\tau = \Phi(s). \tag{4}$$

Using this relationship, it is possible to obtain the full expression of unsteady aerodynamic coefficients in terms of the Theodorsen's function $C(k_n)$ and its circulatory components $F(k_n)$ and $G(k_n)$. It is interesting to note that the reduced frequency parameter k_n for swept and for straight wings coincide:

$$k_n = \frac{\omega b_n}{U_n} = \frac{\omega b \cos\Lambda}{U_\infty \cos\Lambda} = \frac{\omega b}{U_\infty} = k \quad \text{and} \quad i\omega t = ik_n\tau . \tag{5}$$

This implies that the indicial Wagner's function $\phi(\tau)$ remains invariant to any change of the sweep angle.

3. Analytical Developments

For swept wings, the total lift per unit span, can be expressed in the form:

$${}_\Lambda L_a(\bar{y},t) = {}_\Lambda L_c(\bar{y},t) + {}_\Lambda L_{nc1}(\bar{y},t) + {}_\Lambda L_{nc2}(\bar{y},t) + {}_\Lambda L_{nc3}(\bar{y},t). \tag{6}$$

where the indices c and nc identify the various contributions associated with the circulatory and non-circulatory terms, respectively. Using similar notations, the total moment per unit span about the elastic axis is:

$$ {}_{\Lambda}M_a(\bar{y},t)={}_{\Lambda}M_c(\bar{y},t)+{}_{\Lambda}M_{nc1}(\bar{y},t)+{}_{\Lambda}M_{nc2}(\bar{y},t)+{}_{\Lambda}M_{nc3}(\bar{y},t)+{}_{\Lambda}M_{nca}(\bar{y},t), \tag{7} $$

${}_{\Lambda}M_{nca}(\bar{y},t)$ being associated with the apparent moment of inertia[9]. Herein the lift is positive upward, while the moment is positive nose up. For the sake of convenience, herein the plunging coordinate is positive when is downward (see Fig. 1-3). Expressing the vertical displacement Z of a point on the center line of the wing as, (Fig.2):

$$ Z(\bar{x},\bar{y},t)=h(\bar{y},t)+\bar{x}\alpha(\bar{y},t), \tag{8} $$

where $h\equiv h(\bar{y},t)$, $\alpha\equiv\alpha(\bar{y},t)$ are the displacements in plunging and pitching, respectively, and assuming that the origin of the $\bar{x}$ axis coincides with the elastic center, the downwash velocity w normal to the lifting surface becomes:

$$ w(x,y,t)\equiv w(\bar{x},\bar{y},t)=\partial Z/\partial t+U_{\infty}\,\partial Z/\partial\bar{x}\,. \tag{9} $$

The in-plane chordwise coordinate $\bar{x}$ normal to the elastic axis (see Fig. 2) can be expressed as:

$$ \bar{x}=b_n(1/2-a_n). \tag{10} $$

Consequently, using the dimensionless time $\tau(\equiv U_n t/b_n)$ Eq. (9) becomes:

$$ w(\bar{x},\bar{y},\tau)=U_n\left(\frac{h'}{b_n}+\alpha+\frac{\partial h}{\partial\bar{y}}\tan\Lambda+(1/2-a_n)\left(\alpha'+b_n\frac{\partial\alpha}{\partial\bar{y}}\tan\Lambda\right)\right). \tag{11} $$

Herein, b_n is the half-chord of the airfoil, U_n is the component of the flow speed, both normal to the elastic axis and $(\cdot)'\equiv\partial(\cdot)/\partial\tau$. The quantity in Eq. (11) undescored by a solid line is usually discarded in the specialized literature[1,10], as being related to the wing camber effect. However, herein this effect will be taken into consideration.

In the following sections, the unsteady aerodynamic loads in an incompressible flow can be obtained in time (3.1.a) and, with the use of the Laplace transform space in the frequency (3.1.b) domains.

3.1 Unsteady Aerodynamic Loads in Incompressible Flow

3.1.a Time Domain

The circulatory components of the lift expressed in terms of Wagner's indicial function $\phi(\tau)$ (referred also to as *heredity* function) obtained in time domain[9] is:

$$ {}_{\Lambda}L_c(\bar{y},\tau) = -C_{L\alpha_n} b_n \rho U_n^2 \int_{-\infty}^{\tau} \phi(\tau-\tau_0)\left(\frac{h''}{b_n} + \alpha' + \frac{\partial^2 h}{\partial \bar{y}\partial\tau_0}\tan\Lambda + \left(\frac{1}{2} - a_n\right)\left(\alpha'' + b_n \frac{\partial^2 \alpha}{\partial \bar{y}\partial\tau_0}\tan\Lambda \right)\right) d\tau_0, \qquad (12) $$

As concern the aerodynamic non-circulatory components, using the dimensionless time these are expressed as:

$$ {}_{\Lambda}L_{nc1}(\bar{y},\tau) = -\frac{1}{2} C_{L\alpha_n} \rho U_n^2 [h'' - a_n b_n \alpha''], \qquad {}_{\Lambda}L_{nc2}(\bar{y},\tau) = -\frac{1}{2} C_{L\alpha_n} \rho U_n^2 b_n \alpha', $$

$$ {}_{\Lambda}L_{nc3}(\bar{y},\tau) = -\frac{1}{2} C_{L\alpha_n} \rho U_n^2 b_n^2 \tan\Lambda \left[(\delta_r + 1)\frac{\sigma'}{b_n} + \delta_r \lambda + \delta_r \frac{\partial \sigma}{\partial \bar{y}}\tan\Lambda \right] $$

$$ + \frac{1}{2} a_n C_{L\alpha_n} \rho U_n^2 b_n^3 \tan\Lambda \left[(\delta_r + 1)\frac{\lambda'}{b_n} + \delta_r \frac{\partial \lambda}{\partial \bar{y}}\tan\Lambda \right] . \qquad (13) $$

Using the expression of the lift, Eq. (6), the equation for the moment, Eq. (7), can be cast as:

$$ {}_{\Lambda}M_a(\bar{y},t) = -(1/2 + a_n) b_n \, {}_{\Lambda}L_c(\bar{y},t) - a_n b_n \, {}_{\Lambda}L_{nc1}(\bar{y},t) $$

$$ + (1/2 - a_n) b_n \, {}_{\Lambda}L_{nc2}(\bar{y},t) + {}_{\Lambda}M_{nc3}(\bar{y},t) + {}_{\Lambda}M_{nc}(\bar{y},t), \qquad (14) $$

in which the last two non-circulatory components, using the dimensionless time, are expressed as:

$$ {}_{\Lambda}M_{nc3}(\bar{y},\tau) = -\frac{1}{2} C_{L\alpha_n} \rho U_n^2 b_n^3 \frac{1}{2}\lambda \tan\Lambda + \frac{1}{2} C_{L\alpha_n} \rho U_n^2 b_n^3 a_n \tan\Lambda \left[(\delta_r + 1)\frac{\sigma'}{b_n} + \delta_r \lambda \right. $$

$$ \left. + \delta_r \frac{\partial \sigma}{\partial \bar{y}}\tan\Lambda \right] - \frac{1}{2} C_{L\alpha} \rho U_n^2 b_n^4 \left(\frac{1}{8} + a_n^2 \right) \tan\Lambda \left[(\delta_r + 1)\frac{\lambda'}{b_n} + \delta_r \frac{\partial \lambda}{\partial \bar{y}}\tan\Lambda \right], \qquad (15) $$

$$ {}_{\Lambda}M_{nc}(\bar{y},\tau) = -\frac{1}{16} \rho C_{L\alpha_n} b_n^2 U_n^2 \alpha''. \qquad (16) $$

Herein, the spanwise rates of change of bending and twist, σ and λ, respectively, are expressed as $\sigma = \partial h/\partial \bar{y}$ and $\lambda = \partial \alpha/\partial \bar{y}$. In these equations, as well as in the following ones, the terms affected by the tracer δ_r are generated by the last term in the expression of the downwash velocity (Eq. (11)), (term underscored by a solid line). When these terms are discarded, being considered negligibly small, $\delta_r = 0$, otherwise $\delta_r = 1$.

Replacement of Eqs. (12) and (13) in Eq. (6) and of Eqs. (13), (15) and (16) into Eq. (14), results in the unsteady lift and aerodynamic moment expressed in the time domain. Concerning

the circulatory part, Eq. (12), this can be explicitly determined by transforming this expression in the Laplace domain using the relationship between the Laplace transform of the Wagner and Theodorsen functions, namely $C(-is)/s = \mathcal{L}\left(\phi(\tau)\right) = \Phi(s)$ and afterwards inverting back the obtained expression in the temporal space. Alternatively, in order to ease the computations, the available approximate expressions for $\phi(\tau)$ and for $C(k)$[9,11-14] can be used in the Laplace transformed space (see also Ref. 15 where the representation in terms of exponential polynomials and quasi polynomials was used to approximate the supersonic unsteady aerodynamic loads, representation that can be applied also for this case, as well).

The expressions of lift and aerodynamic moment in the time domain, ${}_{\Lambda}L_a(\bar{y},\tau)$ and ${}_{\Lambda}M_a(\bar{y},\tau)$ can be used to determine the subcritical aeroelastic response of swept wings. However, when the aeroelastic response of wings to time-dependent external excitations, such as gusts, sonic-boom, blast pulses, etc. is required, the unsteady aerodynamic loads in the time domain, ${}_{\Lambda}L_a$ and ${}_{\Lambda}M_a$, have to be supplemented by the ones corresponding to above mentioned pulses. This will be considered in the next developments and an illustration of the capabilities provided by this unified method will be given.

3.1.b Frequency Domain

Upon replacing $s \to ik_n$ in the Eqs. (6) and (14) converted in Laplace transformed space; using the relationship between Laplace transform of Wagner and Theodorsen's functions (Eq. (2)); representing the time dependence of displacement quantities as:

$$\alpha(\bar{y},\tau) = f_\alpha(\bar{y})\tilde{\alpha}(\tau,k_n) = f_\alpha(\bar{y})\alpha_0 e^{ik_n\tau}, \qquad h(\bar{y},\tau) = f_h(\bar{y})\tilde{h}(\tau,k_n) = f_h(\bar{y})h_0 e^{ik_n\tau}, \tag{17 a}$$

and expressing:

$${}_{\Lambda}L_a(\bar{y},k_n,\tau) = {}_{\Lambda}\bar{L}_a(\bar{y},k_n)e^{ik_n\tau}, \qquad {}_{\Lambda}M_\alpha(\bar{y},k_n,\tau) = {}_{\Lambda}\bar{M}_\alpha(\bar{y},k_n)e^{ik_n\tau}, \tag{17 b}$$

the equations for the unsteady lift and moment amplitudes can be expressed in the frequency domain (Appendix A). These expressions in the frequency domain can be used in the flutter analysis of swept aircraft wings. These coincide with the ones obtained differently in Ref. 16.
In this analysis $f_\alpha(\bar{y})$ and $f_h(\bar{y})$ are chosen to be the decoupled eigenmodes in plunging and twist of the structure, and are determined as to fulfill identically the boundary conditions. These are expressed as:

$$f_h(\bar{y}) = F_h(\eta \equiv \bar{y}/l) = C_1\left(\frac{\sinh\beta_1 + \sin\beta_1}{\cosh\beta_1 + \cos\beta_1}(\cos\beta_1\eta - \cosh\beta_1\eta) + \sinh\beta_1\eta - \sin\beta_1\eta\right), \tag{18}$$

$$f_\alpha(\bar{y}) = F_\alpha(\eta \equiv \bar{y}/l) = C_2 \sin\beta_2\eta, \tag{19}$$

where for the first bending and torsion we have $\beta_1 = 0.5969\pi$ and $\beta_2 = \pi/2$. The constants C_1 and C_2 are chosen as to normalize $f_h(\bar{y})$ and $f_\alpha(\bar{y})$, and so to get the unitary maximum deflection at the wing tip. The uncoupled first bending and torsion mode shapes were needed for the evaluations of the terms in the Eqs. (A.1) - (A.8) and are shown in Ref. 17.

3.2 Unsteady Aerodynamic Derivatives in the Frequency Domain

In this section close form solution of unsteady aerodynamic coefficients have been derived and their use in the process of unifying the aeroelastic formulations for flutter and response analysis of swept aircraft wings have been emphasized.

A careful inspection of equations for lift and moment expressed in the time domain, Eqs. (7) - (8), suggests the following representations for the lift and aerodynamic moment:

$$_\Lambda L_a(\bar{y}, k_n, \tau) = \frac{1}{2}\rho U_n^2 2b_n\left(k_n H_1\frac{h'}{b_n} + k_n H_2\alpha' + k_n^2 H_3\alpha + k_n^2 H_4\frac{h}{b_n} + H_5\alpha'' + H_6\frac{h''}{b_n}\right), \tag{20}$$

$$_\Lambda M_\alpha(\bar{y}, k_n, \tau) = \frac{1}{2}\rho U_n^2 2b_n^2\left(k_n A_1\frac{h'}{b_n} + k_n A_2\alpha' + k_n^2 A_3\alpha + k_n^2 A_4\frac{h}{b_n} + A_5\alpha'' + A_6\frac{h''}{b_n}\right). \tag{21}$$

Herein, H_i, A_i denote the dimensionless unsteady aerodynamic coefficients, and where k_n has been included as to render the quantities in brackets nondimensional. In a simplified context, such a mixed form of the lift and moment was used in Refs. 18 and 19. The unsteady aerodynamic derivatives for swept wings are obtainable from the previous equations of lift and aerodynamic moment, by assuming harmonic time dependence of displacements quantities. In such a way, the frequency domain counterpart of Eqs. (28) - (29), expressed in compact form, becomes:

$$_\Lambda \bar{L}_a(\bar{y}, k_n) = \rho U_n^2 k_n^2 b_n\left(\frac{h_0}{b_n}L_1 + \alpha_0 L_2\right), \quad _\Lambda \bar{M}_\alpha(\bar{y}, k_n) = \rho U_n^2 k_n^2 b_n^2\left(\frac{h_0}{b_n}M_1 + \alpha_0 M_2\right), \tag{22}$$

Herein, the unsteady aerodynamic complex coefficients L_i and M_i can be expressed in terms of *unsteady aerodynamic derivatives* as:

$$L_1 = i\hat{H}_1 + \hat{H}_4, \qquad L_2 = i\hat{H}_2 + \hat{H}_3, \qquad M_1 = i\hat{A}_1 + \hat{A}_4, \qquad M_2 = i\hat{A}_2 + \hat{A}_3. \tag{23}$$

where, for the sake of convenience, these are written as:

$$\hat{H}_1 = H_1, \hat{H}_2 = H_2, \hat{H}_3 = (H_3 - H_5), \hat{H}_4 = (H_4 - H_6), \tag{24 a}$$

and

$$\hat{A}_1 = A_1, \hat{A}_2 = A_2, \hat{A}_3 = (A_3 - A_5), \hat{A}_4 = (A_4 - A_6). \tag{24 b}$$

The close form solution for the unsteady aerodynamic derivatives in the frequency domain for swept wings will be obtained from Eqs. (22), expressed in terms of Wagner's function $\Phi(ik_n)$. Separating the real and the imaginary parts of these expressions, the unsteady aerodynamic derivatives result under the form displayed in Appendix A. These include also the spanwise rates of change of bending and twist, σ and λ, in terms of derivative in space of the shape functions, which are associated with the sweep effect. For straight wings these terms become immaterial. Notice that, the unsteady aerodynamic loads coincide with the ones obtained differently in Ref. 16, and when specialized for $\delta_r = 0$, with the ones of Ref. 1. The direct use of the aerodynamic derivatives in the Eqs. (20) and (21) will help us to solve the eigenvalue problem associated with determination of the flutter instability. On the other hand, their Laplace transformed counterpart is helpful in the aeroelastic response analysis, wherein the equations of motion are converted to an algebraic systems of equations in the Laplace space. Notice that the flutter analysis can be conducted also in the Laplace space domain. In this case, classical methods such as U-g and p-k methods can be used in the Laplace transformed space.

3.3 Aeroelastic Response of a Swept Wing to Blast and Sonic-Boom Pressure Pulses. Flutter Instability Derived from the Response.

An application on the flutter instability and the aeroelastic response of a swept wing to blast and sonic-boom pressure pulses will be given in the next developments. The aeroelastic governing system of equations of a swept wing featuring plunging and twisting degrees of freedom to blast pressure signatures, expressed in dimensionless form, can be cast as:

$$EI\frac{\partial^4 w}{\partial \bar{y}^4} + m\frac{\partial^2 w}{\partial t^2} - S_y\frac{\partial^2 \theta}{\partial t^2} - L_a(\bar{y},t) = L_b(\bar{y},t), \tag{25}$$

$$GJ\frac{\partial^2 \theta}{\partial \bar{y}^2} + S_y\frac{\partial^2 w}{\partial t^2} - I_y\frac{\partial^2 \theta}{\partial t^2} - M_a(\bar{y},t) = 0. \tag{26}$$

For the cantilevered wing, the related boundary conditions are:

$$\left(w(\bar{y},t) = \frac{\partial w(\bar{y},t)}{\partial \bar{y}} = \theta(\bar{y},t) \right)\Big|_{\bar{y}=0} = 0 \quad \text{and} \quad \left(\frac{\partial^2 w(\bar{y},t)}{\partial \bar{y}^2} = \frac{\partial^3 w(\bar{y},t)}{\partial \bar{y}^3} = \frac{\partial \theta(\bar{y},t)}{\partial \bar{y}} \right)\Big|_{\bar{y}=l} = 0 \qquad (27)$$

Use of shapes functions, given by Eqs. (18) and (19), the aeroelastic governing equations in dimensionless form become:

$$\xi''(\tau) + \bar{\chi}_\alpha \theta''(\tau) + 2\zeta_h (\bar{\omega}/V_n)\xi'(\tau) + (\bar{\omega}/V_n)^2 \xi(\tau) - l_a(\tau) = l_b(\tau), \qquad (28)$$

$$(\bar{\chi}_\alpha / \bar{r}_\alpha^2)\xi''(\tau) + \theta''(\tau) + (2\zeta_\alpha / V_n)\theta'(\tau) + \theta / V_n^2 - m_\alpha(\tau) = 0, \qquad (29)$$

The nondimensional parameters appearing in the preceding equations are displayed in Appendix B. Moreover, all these quantities are based on sections normal to the reference axis.

The dimensionless *sonic-boom* overpressure signature of the N-wave shock pulse, can be expressed as follow:

$$l_b(\tau) = H(\tau)\wp_m \left(1 - \frac{\tau}{\tau_p} \right) - H(\tau - r\tau_p)\wp_m \left(1 - \frac{\tau}{\tau_p} \right). \qquad (30)$$

Herein, the Heaviside step function $H(\tau)$ has been introduced in order to describe the typical pressure time-history for sonic-boom loads; $\wp_m$ denotes the dimensionless peak reflected pressure in excess of the ambient one (see Refs. 4,5,20 and the references therein); τ_p denotes the positive phase duration of the pulse measured from the time of impact of the structure; r denotes the shock pulse length factor. For $r = 1$ the N-shaped pulse degenerates into a triangular pulse that corresponds to an explosive pulse (Fig. 4.a), and for $r = 2$ a symmetric N-shaped pulse is obtained. A depiction of $l_b/\wp_m$ vs. time is displayed in Fig. 4.b.

Equations (28) and (29) can be converted to the Laplace transformed space and solved for the unknowns, $\hat{\xi}$ ($\equiv \mathcal{L}(\xi)$) and $\hat{\theta}$ ($\equiv \mathcal{L}(\theta)$); inverted back in time domain one obtain the plunging and pitching time-histories and the load factor time-history due to the sonic-boom pressure pulse, $\xi(\tau) \equiv \mathcal{L}^{-1}\left(\hat{\xi}(s)\right)$ and $\theta(\tau) \equiv \mathcal{L}^{-1}\left(\hat{\theta}(s)\right)$, respectively. Notice that, in this unified approach, when Eqs. (28) and (29) are converted in the Laplace transformed space, the expressions of aerodynamic derivatives expressed in the Laplace space can be used directly.

Moreover, when the dynamic response of the actively controlled lifting surface is analyzed, also the feedback control forces and moments, that are time dependent, have to be included in Eqs. (25) and (26).

However, when the concept of the boundary feedback control[21-23] is used, the boundary conditions at the wing tip, Eqs. (27) have to be completed by the related control forces or moments.

4. Results and Discussions

Using the idea developed in Ref. 24, a modified strip theory has been developed as to address the problem of the aeroelastic response (for open/closed loop aeroelastic systems), by capturing also the 3-D effects. For swept wings, the local lift-curve slope $C_{L\alpha_n}$ for sections normal to the elastic axis are obtained from the aerodynamics of swept wings[24], and are expressed as

$$C_{L\alpha_n} = C_{L\alpha}/\cos\Lambda \qquad \text{where} \qquad C_{L\alpha} = \frac{C_{L\alpha} AR\cos\Lambda}{\cos\Lambda C_{L\alpha}/\pi + AR\sqrt{1+\left(C_{L\alpha}\cos\Lambda/(\pi AR)\right)^2}},$$

in which also the correction for the aspect ratio AR has been included[10,25].

As a by-product of this analysis, a general close form solution for the unsteady aerodynamic derivative for swept wing are also included. Moreover, in the case in which also the compressibility effects are considered, the respective indicial functions for the compressible subsonic, supersonic and hypersonic flight speed regimes, have to be modified as to include also these effects.

In general, the corrective terms identified by the tracer δ_r do not modify the trend of coefficients. For small aspect ratio wings, the maximum influence of the corrective term is present in the first plunging coefficients $\hat{H}_1$. Usually, for all coefficients, the effect of these terms becomes larger for higher sweep angles and for larger values of the parameter a_n. Whereas, for smaller aspect ratio wings, the effect of the camber becomes significant, and as a result it should be included, for higher aspect ratios, this effect becomes negligibly small.

The aspect ratio AR parameter plays an important role on the coefficients $\hat{H}_4$, $\hat{A}_1$ and $\hat{A}_4$, and because these are correlated to the plunging displacement, the same role will be played on the aerodynamic loads.

Notice that, for $k \to \infty$ the circulatory components of the Theodorsen's function assume the values $F(k) \to 1/2$ and $G(k) \to 0$, and the corresponding unsteady aerodynamic derivatives can be determined, this being in agreement with the steady state solution for lift and aerodynamic

moment. In these developments, all the terms, including the aerodynamic ones associated with $\ddot{h}$ and $\ddot{\alpha}$, have been retained. Usually, these terms are neglected but, due to the presence of high frequency components in the blast pressure terms, their effect can be significant.

As a result, the coefficients H_5, H_6 and A_5, A_6 also subsist. Whereas the aerodynamic coefficients $\hat{H}_1$ and $\hat{A}_2$ are the principal uncoupled aerodynamic damping coefficients in plunging and torsion, respectively, $\hat{H}_2$ and $\hat{A}_1$ are the coupled damping coefficients. As concerns, the depiction of $\hat{H}_i$ and $\hat{A}_i$ versus $2\pi/k$, this representation enables one to get an idea of the variation of the respective quantity with that of the normal freestream speed U_n. It should be mentioned that the expressions of the lift and aerodynamic moment in the frequency domain obtained using the correction of Ref. 16 coincide with the ones obtained here via indicial function approach. These coefficients are directly applied to the flutter analysis and the results are displayed in Fig. 5. The comparison concerns the flutter prediction via indicial function of a cantilever metallic swept wing of $\lambda = 4$ and $\Lambda = 30°$. The results reveal that the predictions provided by the present approach, i.e. $U_F = 235\ ft/s$ and $\omega_F = 386\ rad/s$ are in excellent agreement with those displayed in Ref. 1. In this graph the dotted lines represent the results based on the assumptions in Ref. 1 whereas, the solid line represent those from the present analysis including also the camber effect. The critical value of the flutter speed is obtained here from the eigenvalue analysis of the homogeneous system of equation and at the same time from the response analysis. The way to determine the flutter speed from response becomes clear from the phase plane portrait (see Figs. 11-14), in which, for a certain restricted range of the flight speed (in the vicinity of the flutter speed), a periodic response with constant amplitude is experienced.

On the same figure, determined from the response time-histories, there is also indicated the range in which the flutter instability occurs. The flutter predictions based on both methods show an excellent agreement.

The graphs depicting the aeroelastic response time-history to blast pulses (i.e. explosive and sonic-boom blasts) are displayed in Figs. 6 – 14. In each of these, the corresponding type of blast/gust signature was indicated as an inset. In addition, the parameters in use for the simulations, unless otherwise specified, are chosen as: V_n=1; μ = 10; $\bar{\omega}$ = 0.5; $r_\alpha = 0.5$;$\chi_\alpha = 0.125$;

$\zeta_\eta = \zeta_\alpha = 0; a_n$=-0.2) and ($\wp_m$=1;$\tau_p$ =15";r=1 or 2) for the structural and the load components, respectively.

In Fig. 6 predictions of the aeroelastic response of a straight/swept wings to a gust load (indicated in the inset of the figure) are presented. Within this plot both the exact and selected approximate expressions of the Theodorsen's function (Ref. 1) are used. As is readily seen, the differences occurring as a result of these approximations in the plunging time-history are indiscernible, which allows us to infer about the high accuracy of the approximations involving the expression of $C(s)$. Nevertheless, for more complex wing configurations these approximate expressions can be highly useful towards determining the aeroelastic response.

The graphs in Fig. 7 supply the dimensionless plunging $(\xi \equiv w/b_n)$ and pitching (θ) displacements, and the load factor ($N \equiv 1 + w''/g$, where g is the acceleration of gravity) time-history aeroelastic responses to blast pressure pulse. It becomes apparent that an increase of the wing sweep angle, results in a decrease of the severity of the pulse signature.

Moreover, the plunging-pitching coupling helps to reduce the amplitude of the aeroelastic response[17]. The load factor N has its maximum for τ = 0, when the first impulse due the blast load occurs.

Figures 8 highlights the effect of the speed parameter V_n $(\equiv U_n/b_n\omega_\alpha)$ on the swept aircraft wing (Λ = 15°) subjected to blast pulses. It becomes apparent that the amplitude of the response time-history increases with the increase of V_n. Moreover, in a certain range of speeds, as time unfolds, a decay of the amplitude is experienced, which reflects the fact that in this case the subcritical response is involved. However, for the dimensionless speed parameter $V_n \cong 2.1$, the response becomes unbounded implying that the occurrence of the flutter instability is impending. The effect of the mass parameter μ $\left(\equiv m/\pi\rho b_n^2\right)$ for swept wing of Λ = 15° is indicated in Figs. 9. The increase of the mass ratio and consequently of the aspect ratio *AR*, (see Appendix A) results in the increase of the plunging and pitching displacement amplitudes. Moreover, for higher mass ratios and *AR*, the motion damps out at larger times.

It should be noticed that the response to sonic-boom pressure pulses involves two different regimes (see Fig. 10); namely: one for which $0 < \tau < 30$" that corresponds to the forced motion, and the other one to $\tau > 30$" belonging to the free motion. The jump in the time-history of N is due to the discontinuity in the load occurring at $\tau = 30$". This jump doesn't appear for explosive

pressure pulses, where r = 1 (see Figs. 7-9). Moreover, also in this case, when increasing the sweep angle, the effect of the blast signature becomes less severe. In Fig. 11 a three-dimensional plot depicting the dimensionless plunging ξ and pitching θ deflection time-histories of a swept aircraft wing ($\Lambda = 15^{o}$) to blast pressure signatures vs. the normalized spanwise coordinate y and the dimensionless time τ has been supplied for two different values of the dimensionless speed parameter V_n , 1.00 and 2.5.

The evolution of the aeroelastic system can be graphically illustrated by examining its motion in the *phase – space*, rather than in the real space, and recognizing that the trajectory depicted in this space represents the complete time history of the system. Corresponding to the flutter speed, that coincides with that otained from the eigenvalue analysis, the trajectory of motion describes an orbit with constant amplitude, the so called center. For $V < V_F$ as time unfolds, a decay of the amplitude is experienced, which reflects the fact that in this case a subcritical response is involved (stable focal point), while for $V > V_F$ the response becomes unbounded implying that the occurrence of the flutter instability is impending (unstable focal point).

Figure 12 highlights a three dimensional phase space portrait (ξ vs. $\dot{\xi}$ and N) of the plunging time-history response to blast load of a swept aircraft wing ($\Lambda = 15^{o}$) for selected values of the speed parameter. As it is shown, the response becomes unbounded for $V_n \cong 2.1$, representing the critical speed in which the periodic solution has been obtained and implying that the occurrence of the flutter instability is impending. To avoid its occurrence there are two possibilities, namely, including a passive/active control methodology or acting on the sweep angle Λ. In the latter case the idea is to use the capabilities of the aircraft featuring variable sweep angle (e.g. *F-14 Tomcat*) as to reduce the oscillations and at the same time expand the flight envelope.

Figure 13 shows the phase plane portrait and the relative 3-D plots (vs. the load factor N) for selected values of the sweep angle Λ. With the increase of the sweep angle, the motion damps out at smaller times, the amplitude of the response is lower and the load factor is lower as well.

In Figs. 14 a 3-D pictorial view of the motions in plunging and pitching around the flutter instability boundary vs. the variation of the sweep angle are displayed. From these plots a complete view of how the maximum maximorum of the admissible values of the amplitudes as

function of the sweep angle are evolving. It clearly appears that acting on an aircraft featuring swept wing angle variability, the subcritical aeroelastic response can be controlled in terms of the plunging and pitching displacement amplitudes.

5. Conclusions

An unified treatment of the aeroelasticity of swept lifting surfaces in time and frequency domains has been presented, and the usefulness, in this context, of the aerodynamic indicial functions concept was emphasized. The time domain representation is essential towards determination of the dynamic aeroelastic response to time dependent external loads, and in the case of the application of a feedback control methodology, of the dynamic aeroelastic response to both external time dependent loads and control inputs. The aeroelastic response have been represented in both, the classical way, by displaying the time-histories of plunging – pitching and load factor, and in an original *phase – space* context, that provides full information about the behavior of the aeroelastic system. The frequency domain representation is essential towards determination of the flutter instability. It was also shown how to capture the flutter instability also from the response time-histories. In this sense, the inclusive approach used here will be helpful toward the validation of the aeroelastic model via the comparison of the theoretical and flight vibration test results[26].

Applications assessing the versatility of the methodology presented here toward the approach of both the subcritical aeroelastic responses and flutter instability for 3-D swept aircraft wing have been presented. The concept of the stability boundary and control of it via the use of the variable-sweep-wing-geometry have been illustrated. The unified formulation presented in this work can be extended as to approach it in various flight speed regimes[27-30] and to include also a feedback control mechanism. Moreover, the methodology developed in this paper can assist determination of the critical flutter speed from the investigation in flight or in wind tunnel tests of the aeroelastic response of aircraft wings to pulse loading.

Acknowledgment

The work reported here was partially supported by NASA Langley Research Center through Grant NAG-1-2281.

References

[1] Bisplinghoff, R.L., Ashley, H., and Halfman R.L., *Aeroelasticity*, Dover Publications, Inc., New York, 1996.

[2] Lomax, H., "Indicial Aerodynamics," Part II, Chapter 6. AGARD Manual on Aeroelasticity.

[3] Tobak, M., "On the use of the indicial Function Concept in the Analysis of Unsteady Motion of Wings and Wing-Tail Combinations," NASA Report. 1188, 1954.

[4] Librescu, L., and Nosier, A., "Response of Laminated Composite Flat Panels to Sonic-Boom and Explosive Blast Loading," *AIAA Journal*, Vol. 28, No. 2, pp. 345-352, 1990.

[5] Librescu, L., and Na, SS., "Dynamic Response of Cantilevered Thin-Walled Beams to Blast and Sonic-Boom Loadings," *Journal of Shock and Vibration*, Vol. 5, No. 1, 1998, pp. 23-33.

[6] Karpel, L. Design for active flutter suppression and gust alleviation using state-space aeroelastic modeling, *Journal of Aircraft*, Vol. 19, No. 3, 1982, pp. 221-227.

[7] Roger, K.L., "Airplane Math Modeling Methods for Active Control Design," AGARD-CP-228, August 1977.

[8] Edwards, J.W., Ashley, H., and Breakwell, J.V., "Unsteady Aerodynamic Modeling for Arbitrary Motions," *AIAA Journal*, Vol. 17, No. 4, 1979, pp. 365-374, presented as AIAA Paper 77-451 at the AIAA Dynamics Specialist Conference, San Diego, California, 1977.

[9] Fung, Y.C., *An introduction to the Theory of Aeroelasticity*, John Wiley, New York, NY, 1955.

[10] Flax, A.H., "Aeroelasticity and Flutter, in High Speed Problems of Aircraft and Experimental Methods," *High Speed Aerodynamics and Jet Propulsion*, Vol. VIII, Eds. Donovan, H.F. and Lawrence, H.R., Princeton University Press, 1961, pp. 161-417.

[11] Eversman, W., and Tewari, A., "Modified Exponential Series Approximation for the Theodorsen Function," *Journal of Aircraft*, Vol. 28, No. 9, pp. 553-557, 1991.

[12] Queijo, M.J., Wells, W.R., and Keskar, D.A., "Approximate Indicial Lift Function for Tapered, Swept Wings in Incompressible Flow," NASA TP-1241, pp. 30, 1978.

[13] Venkatesan, C., and Friedmann, P.P., "New Approach to Finite-State Modeling of Unsteady Aerodynamics," *AIAA Journal*, Vol. 24, No. 12, pp. 1889-1897, 1986.

[14] Tewari, A., and Spalink, J.B., "Multiple Pole Rational-Function Approximations for Unsteady Aerodynamics," *Journal of Aircraft*, Vol. 30, No. 3, pp. 426-428, Engineering Note, 1993.

[15]Librescu, L., "Unsteady Aerodynamic Theory of Lifting Surfaces and Thin Elastic Bodies Undergoing Arbitrary Small Motions in a Supersonic Flow Field," *Quarterly Journal of Mechanics and Applied Mathematics*, Vol. 40, Pt. 4, 1987, pp. 539 –557.

[16]Barmby, J.G., Cunningham, H.J., and Garrick, I.E., "Study of Effects of Sweep on the Flutter of Cantilever Wings," NACA Report No. 1014, 1951.

[17]Marzocca, P., Librescu, L., and Silva, W.A., "Aerodynamic Indicial Functions and Their Use in Aeroelastic Formulation of Lifting Surfaces," presented as AIAA-2000-WIP at the 41st AIAA/ASME/ASCE/AHS/ASC Structures, Structural Dynamics, and Materials Conference, Atlanta, Georgia, 2000.

[18]Simiu, E., and Scanlan, R.H., "Wind Effects on Structures," *An Introduction to Wind Engineering*, 2nd Ed., John Wiley, NY, 1986.

[19]Scanlan, R.H., "Aeroelastic Problems of Civil Engineering Structures," *A Modern Course in Aeroelasticity*, Dowell, E.H. editor, Kluwer Academic Publishers, Third Revised and Enlarged Edition, 1996.

[20]Department of the Army, Fundamentals of Protective Design for Conventional Weapons, Technical Manual TM 5-855-1, November 1986.

[21]Librescu, L., Meirovitch, L., and Na, S.S., "Control of Cantilevers Vibration Via Structural Tailoring and Adaptive Materials," *AIAA Journal*, Vol. 35, No. 8, 1997, pp. 1309-1315.

[22]Librescu, L., and Na, S.S., "Bending Vibration Control of Cantilevers Via Boundary Moment and Combined Feedback Control Laws," *Journal of Vibration and Controls*, Vol. 4, No. 6, 1998, pp. 733-746.

[23]Librescu, L., and Gern, F.H., "Synergistic Interaction of Aeroelastic Tailoring and Boundary Moment Control on Aircraft Wing Flutter" NASA/CP-1999-209136/PT 2 CEAS/ AIAA/ICASE/NASA International Forum on Aeroelasticity and Structural Dynamics, June 1999, pp. 719-733.

[24]Yates, C., "Calculation of Flutter Characteristics for Finite-Span Swept or Unswept Wings at Subsonic and Supersonic Speeds by a Modified Strip Analysis," NACA RM No. L57L10, 1958.

[25]Bisplinghoff, R.L., and Ashley, H., *Principles of Aeroelasticity*, Dover Publications, Inc., New York, 1975.

[26]Lacabanne, M., and Esquerre, J.P., "Correlation Between Theoretical Flutter Models and Tests for Civil Aircraft," Aerospatiale–Aircraft Division Technical report, 1995.

[27]Mazelsky, B., "Numerical Determination of Indicial Lift of a Two-Dimensional Sinking Airfoil at Subsonic Mach Numbers from Oscillatory Lift Coefficients with Calculations for Mach Number 0.7," NACA-TN-2562, December 1951 and NACA-TN-2613, February 1952.

[28]Lomax, H., Heaslet, M.A. & Sluder, L., "The Indicial Lift and Pitching Moment for a Sinking or Pitching Two-Dimensional Wing Flying at Subsonic or Supersonic Speeds," NACA-TN-2403, July 1951.

[29]Beddoes, T.S., "Practical Computation of the Unsteady Lift," *Vertica*, Vol. 8, No. 1, 1984, pp. 55-71.

[30]Leishman, J.G., "Validation of Approximate Indicial Aerodynamic Functions for Two-dimensional Subsonic Flow," *Journal of Aircraft*, Vol. 25, No. 10, 1988, pp. 914-922.

Appendix A

Unsteady Aerodynamic Derivatives:

$$\hat{H}_1 = -C_{L\alpha_n}\left(\frac{F(k_n)}{k_n} f_h + \left(\frac{G(k_n)}{k_n} + \frac{1}{2}(1+\delta_r)\right)\frac{1}{k_n}\frac{\partial f_h}{\partial \eta}\frac{\sin\Lambda}{2AR}\right), \tag{A.1}$$

$$\hat{H}_2 = -\frac{C_{L\alpha_n}}{k_n}\left(\left(\left(\frac{1}{2}-a_n\right)F(k_n)+\frac{G(k_n)}{k_n}+\frac{1}{2}\right)f_\alpha + \left(\frac{2G(k_n)}{k_n}\left(\frac{1}{2}-a_n\right)-\frac{1}{2}a_n(1+\delta_r)\right)\frac{\partial f_\alpha}{\partial \eta}\frac{\sin\Lambda}{2AR}\right), \tag{A.2}$$

$$\begin{aligned}\hat{H}_3 = -C_{L\alpha_n}&\left(\left(\frac{F(k_n)}{k_n^2} - \frac{G(k_n)}{k_n}\left(\frac{1}{2}-a_n\right)+\frac{1}{2}a_n\right)f_\alpha\right.\\ &\left.+\left(F(k_n)\left(\frac{1}{2}-a_n\right)+\frac{1}{2}\delta_r\right)\frac{1}{k_n^2}\frac{\partial f_\alpha}{\partial \eta}\frac{\sin\Lambda}{2AR} - \delta_r\frac{1}{2}\frac{1}{k_n^2}\frac{\partial^2 f_\alpha}{\partial \eta^2}a_n\left(\frac{\sin\Lambda}{2AR}\right)^2\right),\end{aligned} \tag{A.3}$$

$$\hat{H}_4 = C_{L\alpha_n}\left(\left(\frac{1}{2}+\frac{G(k_n)}{k_n}\right)f_h - \left(F(k_n)\frac{\partial f_h}{\partial \eta}+\delta_r\frac{1}{2}\frac{\partial^2 f_h}{\partial \eta^2}\frac{sc}{AR}\right)\frac{1}{k_n^2}\frac{\sin\Lambda}{2AR}\right), \tag{A.4}$$

$$\hat{A}_1 = \frac{C_{L\alpha_n}}{k_n}\left(\left(\frac{1}{2}+a_n\right)F(k_n)f_h + \left(\left(\frac{1}{2}+a_n\right)\frac{G(k_n)}{k_n}+\frac{1}{2}a_n(\delta_r+1)\right)\frac{\partial f_h}{\partial \eta}\frac{\sin\Lambda}{2AR}\right), \tag{A.5}$$

$$\begin{aligned}\hat{A}_2 = \frac{C_{L\alpha_n}}{2k_n}&\left(\left(\left(a_n-\frac{1}{2}\right)+\left(\frac{1}{2}+a_n\right)\frac{2G(k_n)}{k_n}-\left(a_n^2-\frac{1}{4}\right)2F(k_n)\right)f_\alpha\right.\\ &\left.+\left(\left(\frac{1}{4}-a_n^2\right)\frac{2G(k_n)}{k_n}-(\delta_r+1)\left(\frac{1}{8}+a_n^2\right)\right)\frac{\partial f_\alpha}{\partial \eta}\frac{\sin\Lambda}{2AR}\right),\end{aligned} \tag{A.6}$$

$$\begin{aligned}\hat{A}_3 = \frac{C_{L\alpha_n}}{4k_n^2}&\left(\left((1+2a_n)2F(k_n)+(4a^2-1)G(k_n)k_n+\left(2a_n^2+\frac{1}{4}\right)k_n^2\right)f_\alpha\right.\\ &\left.+\left(\left(1-4a_n^2\right)F(k_n)-(1-\delta_r 2a_n)\right)\frac{\partial f_\alpha}{\partial \eta}\frac{\sin\Lambda}{2AR}-\delta_r\left(\frac{1}{4}+2a_n^2\right)\frac{\partial^2 f_\alpha}{\partial \eta^2}\left(\frac{\sin\Lambda}{2AR}\right)^2\right),\end{aligned} \tag{A.7}$$

$$\hat{A}_4 = -C_{L\alpha_n}\left(\left(\frac{1}{2}a_n+\left(\frac{1}{2}+a_n\right)\frac{G(k_n)}{k_n}\right)f_h - \left(\left(\frac{1}{2}+a_n\right)F(k_n)\frac{\partial f_h}{\partial \eta}+\delta_r\frac{1}{2}a_n\frac{\partial^2 f_h}{\partial \eta^2}\frac{\sin\Lambda}{2AR}\right)\frac{1}{k_n^2}\frac{\sin\Lambda}{2AR}\right). \tag{A.8}$$

where the aspect ratio AR is defined as $AR = l_n/b_n\cos^2\Lambda$ and the spanwise dimensionless coordinate $\eta = \bar{y}/l$ have been introduced. For $\Lambda = 0$ the expressions of aerodynamic coefficients corresponding to straight wings are obtained.

Appendix B

Nondimensional parameters for flutter and response analyses:

$$l_a = \frac{L_a b_n}{m U_n^2 \left(\int_0^1 f_h^2 d\eta \right)}; \qquad m_a = M_\alpha b_n^2 \Big/ \left(I_y U_n^2 \int_0^1 f_\alpha^2 d\eta \right); \qquad V_n = U_n / b_n \omega_\alpha ;$$

$$\wp_m = \frac{P_m b_n}{m U_n^2 \left(\int_0^1 f_h^2 d\eta \right)}; \qquad \mu = m / C_{L\alpha} \rho b_n^2 ; \qquad \zeta_h = c_h / 2 m \omega_h ;$$

$$\xi = h / b_n ; \qquad \zeta_\alpha = c_\alpha / 2 I_\alpha \omega_\alpha ; \qquad \overline{\omega} = \omega_h / \omega_\alpha ;$$

$$\overline{r}_\alpha^2 = I_y / m b_n^2 \left(\int_0^1 f_\alpha^2 d\eta \Big/ \int_0^1 f_h^2 d\eta \right); \qquad \overline{\chi}_\alpha = \frac{S_\alpha}{mb} \left(\int_0^1 f_\alpha f_h d\eta \Big/ \int_0^1 f_h^2 d\eta \right);$$

Figure Captions

Fig. 1 Nonuniform swept wing.

Fig. 2 Airfoil section.

Fig. 3 3-D view of a swept wing.

Fig. 4 (a) Sonic-Boom and (b) Triangular Blast Pressure Pulses.

Fig. 5 Flutter calculation via U-g method (Ref. 1).

Fig. 6 Predictions of the aeroelastic responses of a straight/swept wings to a gust load, based on exact and selected expressions of the Theodorsen's function.

Fig. 7 Influence of angle of sweep Λ on the aeroelastic response to a blast pressure pulse at the wing tip.

Fig. 8 Influence of the speed parameter V_n on the response of a swept aircraft wing ($\Lambda = 15^o$) to blast pulses at the wing tip.

Fig. 9 Influence of the mass parameter μ on the response of a swept aircraft wing ($\Lambda = 15^o$) to blast pulses at the wing tip.

Fig. 10 Influence of the sweep angle Λ on the response to sonic-boom pulses at the wing tip.

Fig. 11 Three-dimensional plots depicting the dimensionless plunging ξ and pitching θ deflection time-history of a swept aircraft wing ($\Lambda = 15^o$) to blast pressure signature, vs. the normalized spanwise coordinate y and the dimensionless time τ.

Fig. 12 Three-dimensional phase-space portrait depicting the dimensionless plunging deflection time-history of a swept aircraft wing ($\Lambda = 15^o$) to blast pressure signature, vs. the load factor N for selected values of the speed parameter.

Fig. 13 Phase-plane $(\xi;\dot{\xi})$ and phase-space portraits $(\xi;\dot{\xi};N)$ depicting the dimensionless plunging deflection time-history of a swept aircraft wing to blast pressure signature, for selected values of the sweep angle.

Fig. 14 Cone of stability orbits depicting the envelope of the upper bound values of the dimensionless plunging and pitching deflection time-histories vs. Λ to blast pressure signatures.

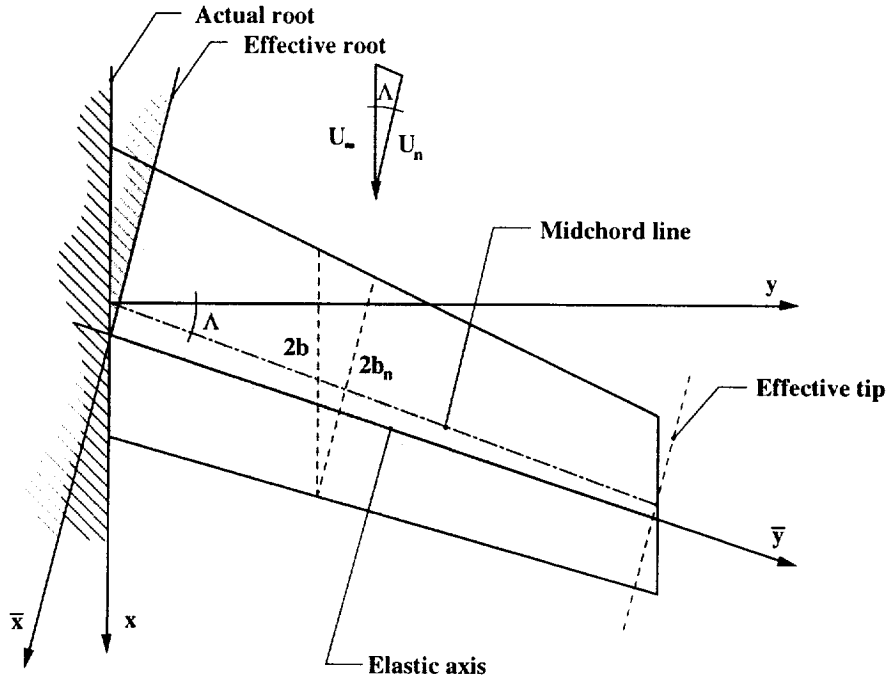

Fig. 1

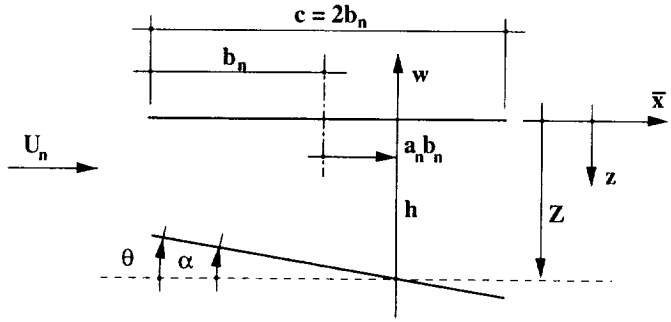

Fig. 2

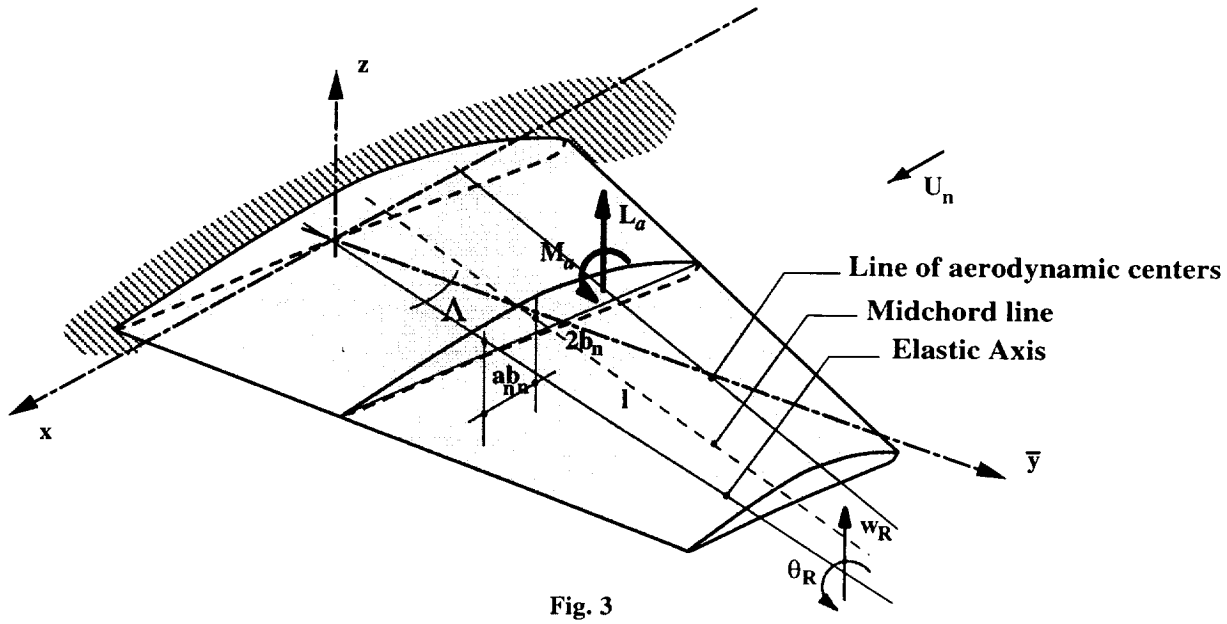

Fig. 3

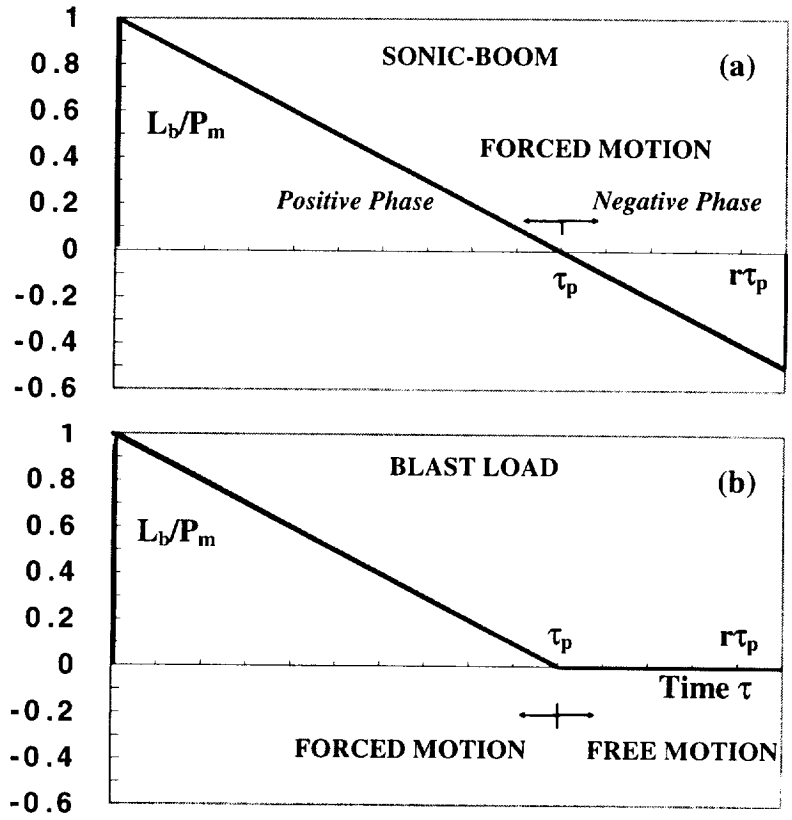
1
0.8
0.6
0.4
0.2
0
-0.2
-0.4
-0.6
SONIC-BOOM
(a)
L_b/P_m
FORCED MOTION
Positive Phase
Negative Phase
τ_p
$r\tau_p$
1
0.8
0.6
0.4
0.2
0
-0.2
-0.4
-0.6
BLAST LOAD
(b)
L_b/P_m
τ_p
$r\tau_p$
Time τ
FORCED MOTION
FREE MOTION

Fig. 4

Flutter Analysis: U–g Method

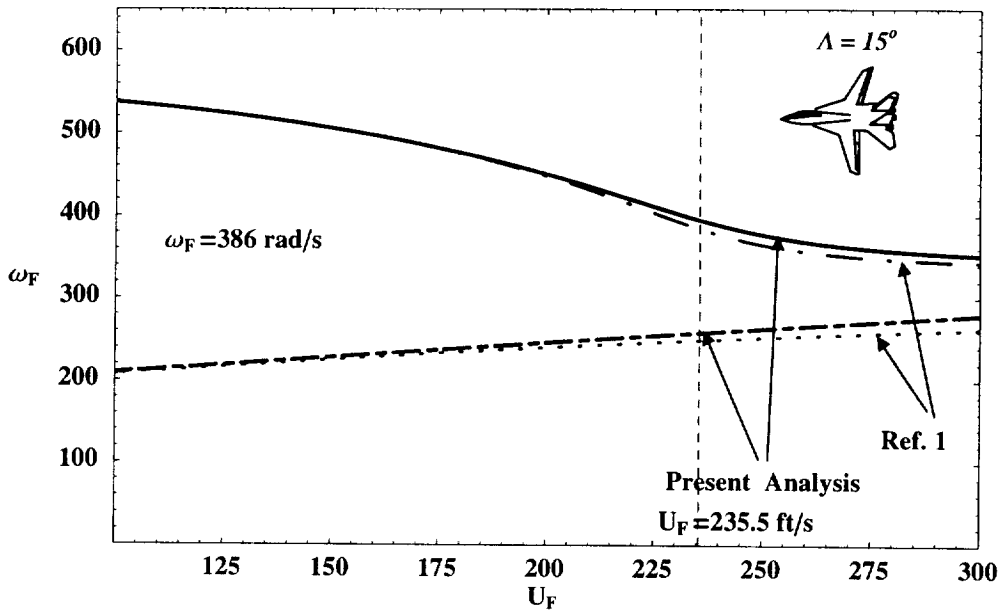

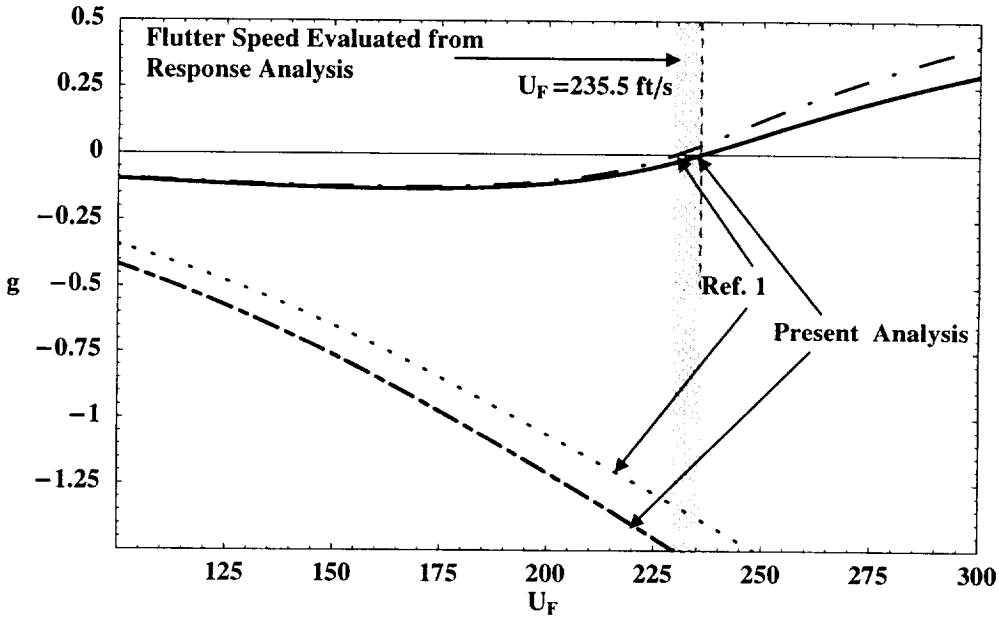

Fig. 5

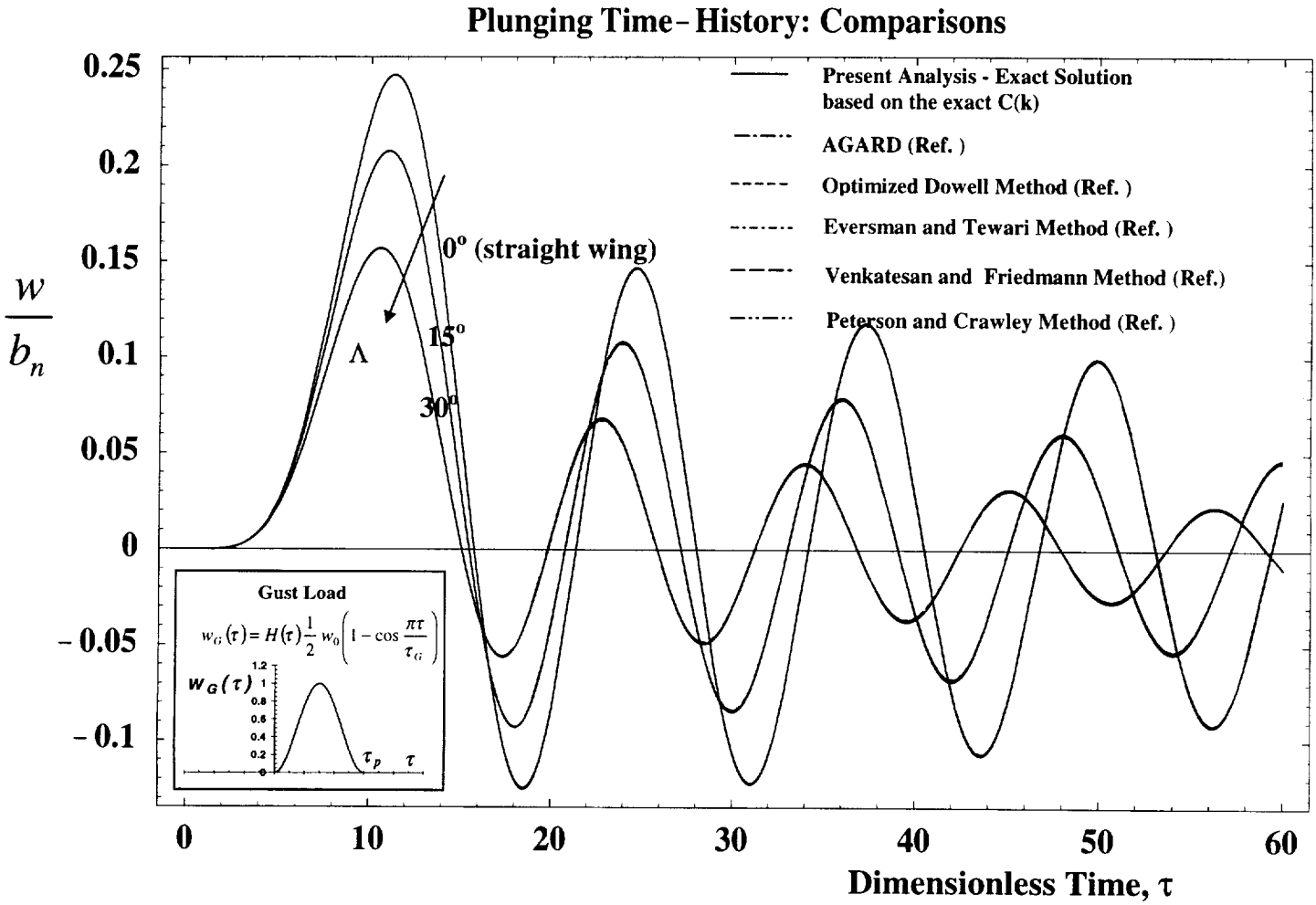
Plunging Time-History: Comparisons
0.25
0.2
0.15
0.1
0.05
0
-0.05
-0.1
w/b_n
0
10
20
30
40
50
60
Dimensionless Time, τ
Present Analysis - Exact Solution based on the exact C(k)
AGARD (Ref.)
Optimized Dowell Method (Ref.)
Eversman and Tewari Method (Ref.)
Venkatesan and Friedmann Method (Ref.)
Peterson and Crawley Method (Ref.)
0° (straight wing)
Λ
15°
30°
Gust Load
w_G(τ) = H(τ) 1/2 w_0 (1 - cos πτ/τ_G)
w_G(τ)
τ_p
τ

Fig. 6

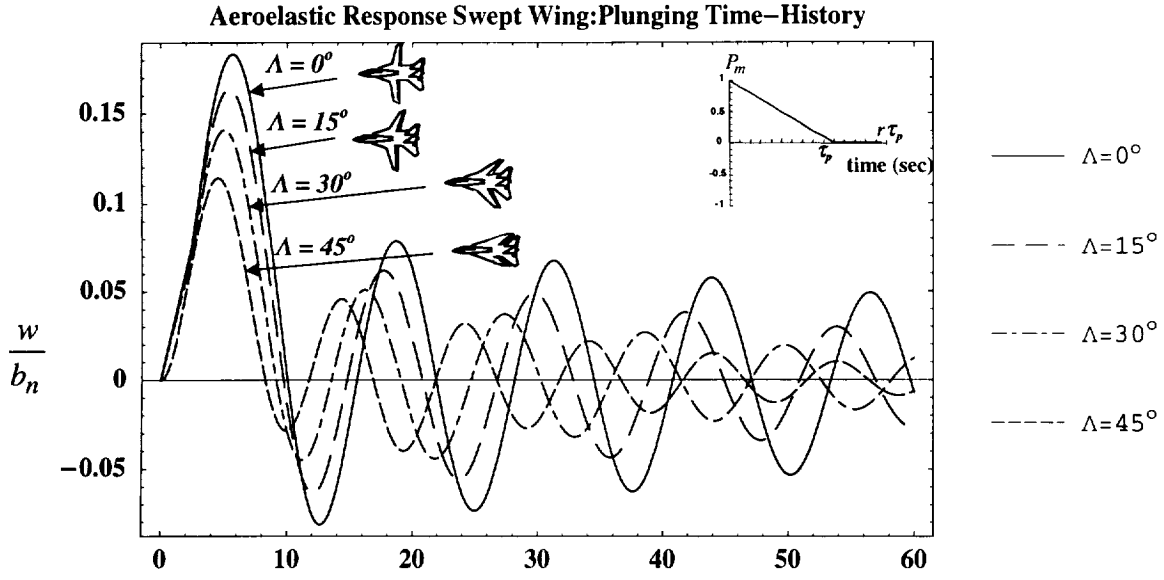
Aeroelastic Response Swept Wing:Plunging Time–History
Λ = 0°
Λ = 15°
Λ = 30°
Λ = 45°
P_m
$r\tau_p$
τ_p
time (sec)
$\frac{w}{b_n}$
0.15
0.1
0.05
0
−0.05
0
10
20
30
40
50
60
Λ=0°
Λ=15°
Λ=30°
Λ=45°

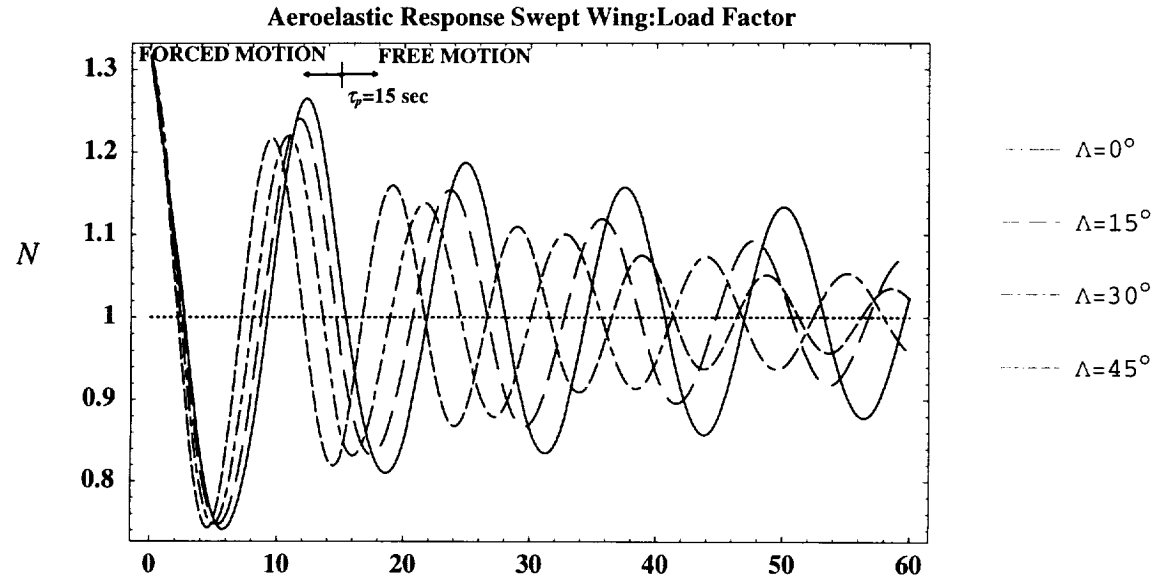
Aeroelastic Response Swept Wing:Load Factor
FORCED MOTION
FREE MOTION
τ_p=15 sec
N
1.3
1.2
1.1
1
0.9
0.8
0
10
20
30
40
50
60
Λ=0°
Λ=15°
Λ=30°
Λ=45°

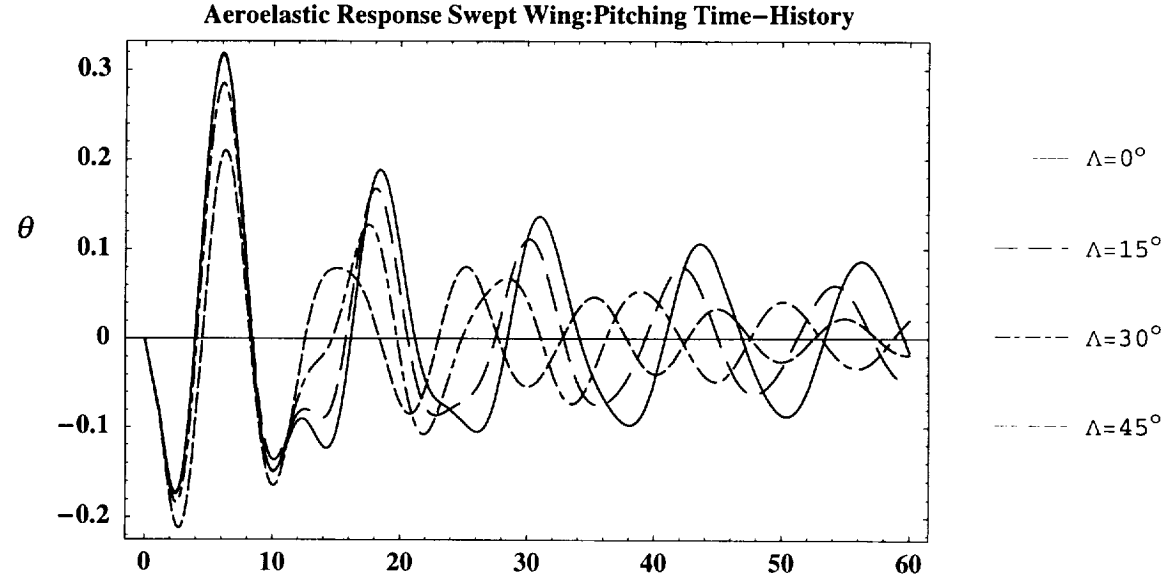
Aeroelastic Response Swept Wing:Pitching Time–History
θ
0.3
0.2
0.1
0
−0.1
−0.2
0
10
20
30
40
50
60
Λ=0°
Λ=15°
Λ=30°
Λ=45°

Fig. 7

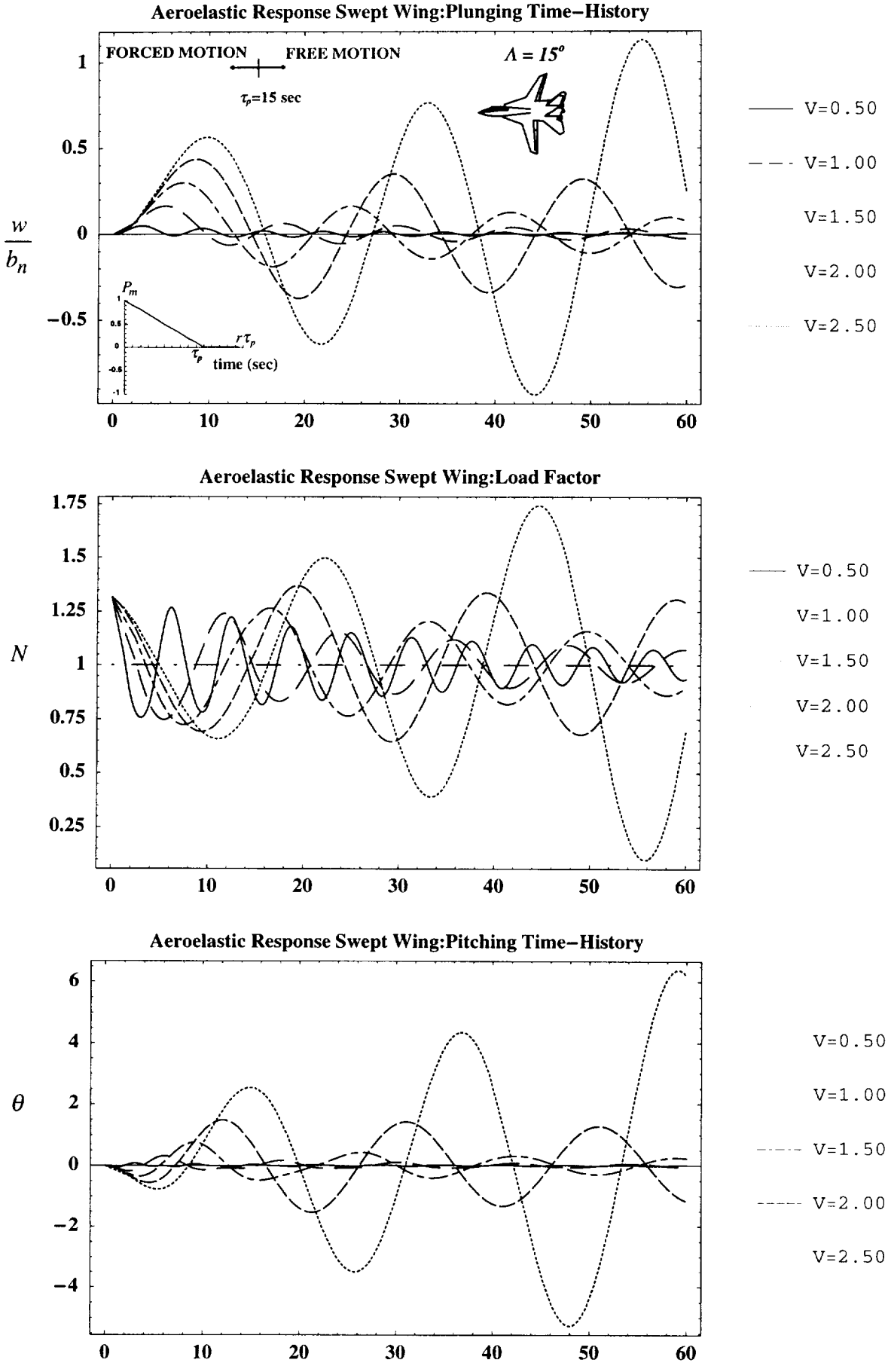
Aeroelastic Response Swept Wing:Plunging Time–History
FORCED MOTION
FREE MOTION
τ_p=15 sec
$\Lambda = 15^o$
$\frac{w}{b_n}$
P_m
$r\tau_p$
τ_p
time (sec)
V=0.50
V=1.00
V=1.50
V=2.00
V=2.50
Aeroelastic Response Swept Wing:Load Factor
N
V=0.50
V=1.00
V=1.50
V=2.00
V=2.50
Aeroelastic Response Swept Wing:Pitching Time–History
θ
V=0.50
V=1.00
V=1.50
V=2.00
V=2.50

Fig. 8

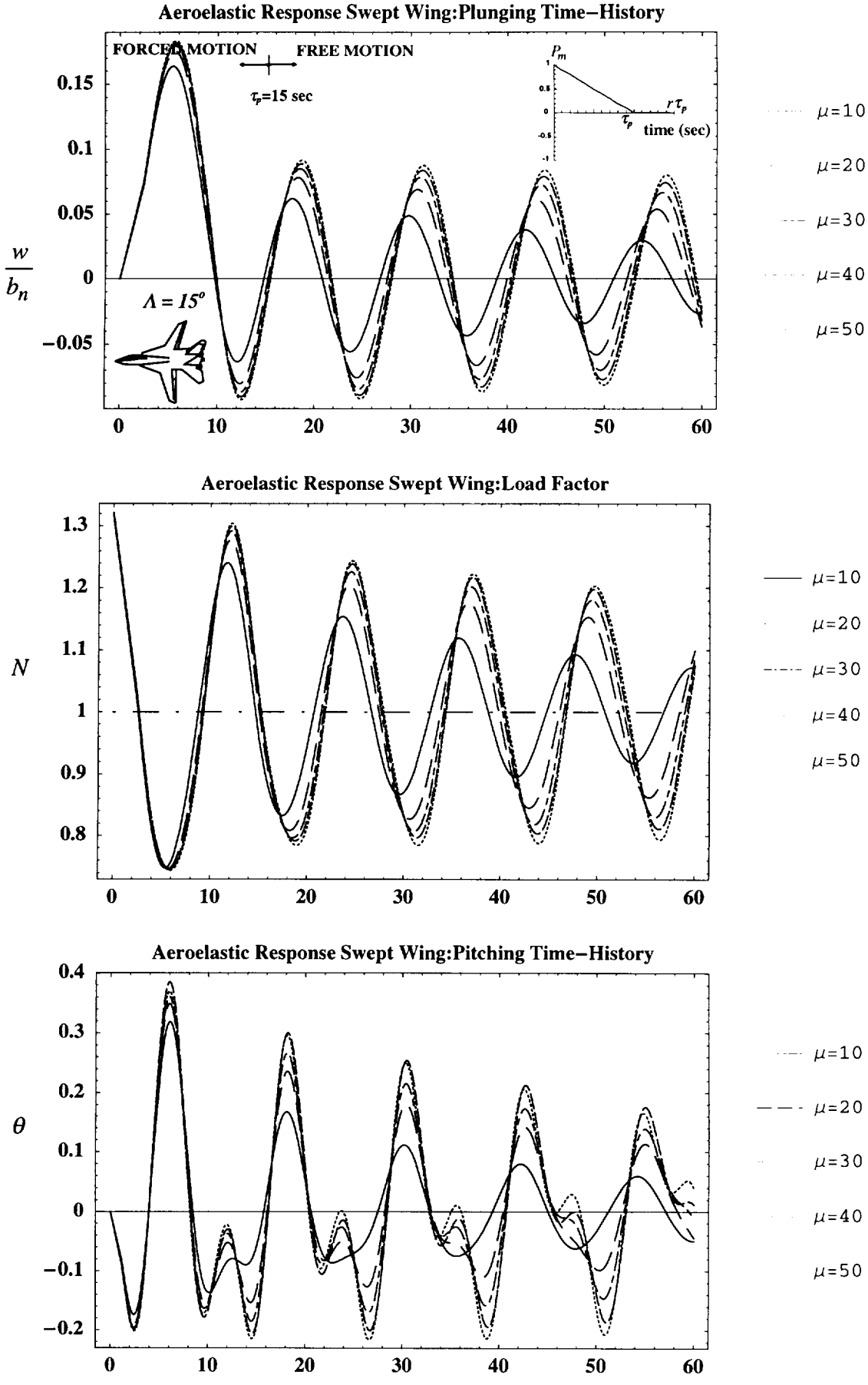
Aeroelastic Response Swept Wing:Plunging Time–History
FORCED MOTION
FREE MOTION
τ_p=15 sec
P_m
$r\tau_p$
τ_p
time (sec)
$\frac{w}{b_n}$
$\Lambda = 15^o$
0.15
0.1
0.05
0
−0.05
0
10
20
30
40
50
60
μ=10
μ=20
μ=30
μ=40
μ=50
Aeroelastic Response Swept Wing:Load Factor
N
1.3
1.2
1.1
1
0.9
0.8
0
10
20
30
40
50
60
μ=10
μ=20
μ=30
μ=40
μ=50
Aeroelastic Response Swept Wing:Pitching Time–History
θ
0.4
0.3
0.2
0.1
0
−0.1
−0.2
0
10
20
30
40
50
60
μ=10
μ=20
μ=30
μ=40
μ=50

Fig. 9

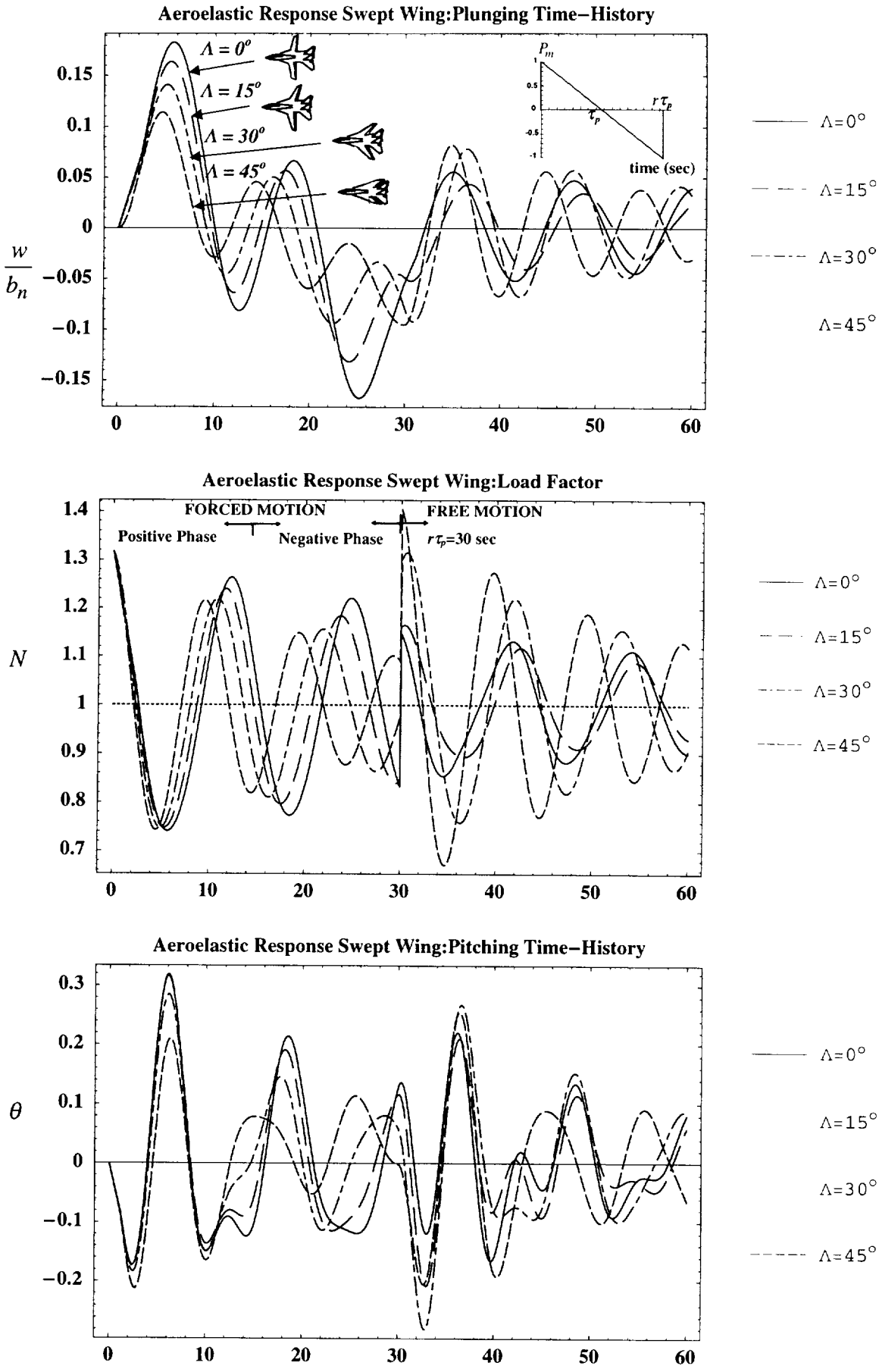
Aeroelastic Response Swept Wing:Plunging Time–History
Λ = 0°
Λ = 15°
Λ = 30°
Λ = 45°
time (sec)
w/b_n
Λ=0°
Λ=15°
Λ=30°
Λ=45°
Aeroelastic Response Swept Wing:Load Factor
FORCED MOTION
FREE MOTION
Positive Phase
Negative Phase
rτ_p=30 sec
N
Λ=0°
Λ=15°
Λ=30°
Λ=45°
Aeroelastic Response Swept Wing:Pitching Time–History
θ
Λ=0°
Λ=15°
Λ=30°
Λ=45°

Fig. 10

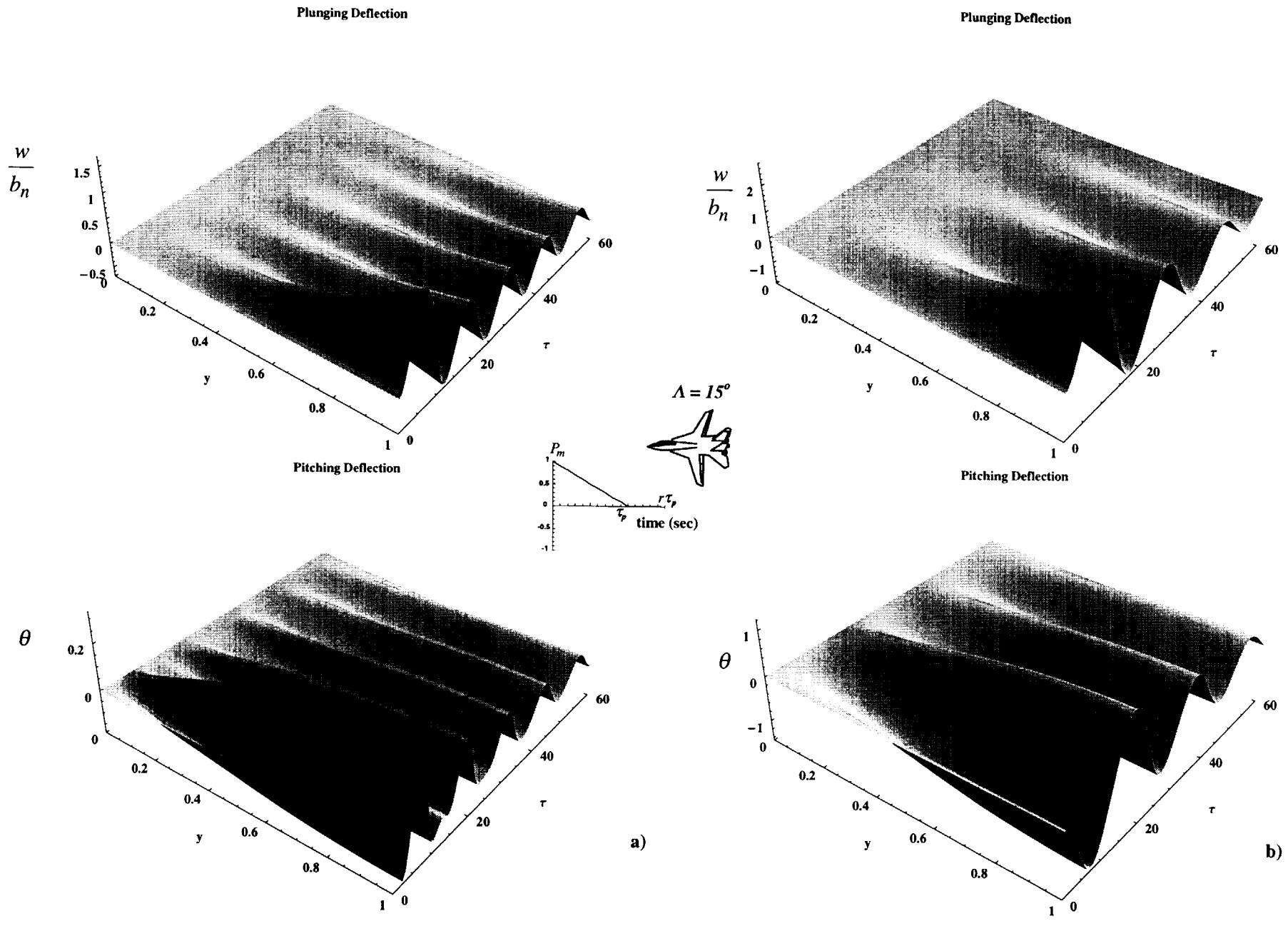

$V_n = 1.00$

$V_n = 2.50$

Fig. 11

3D Phase Space Portrait – $\Lambda = 15^{o}$

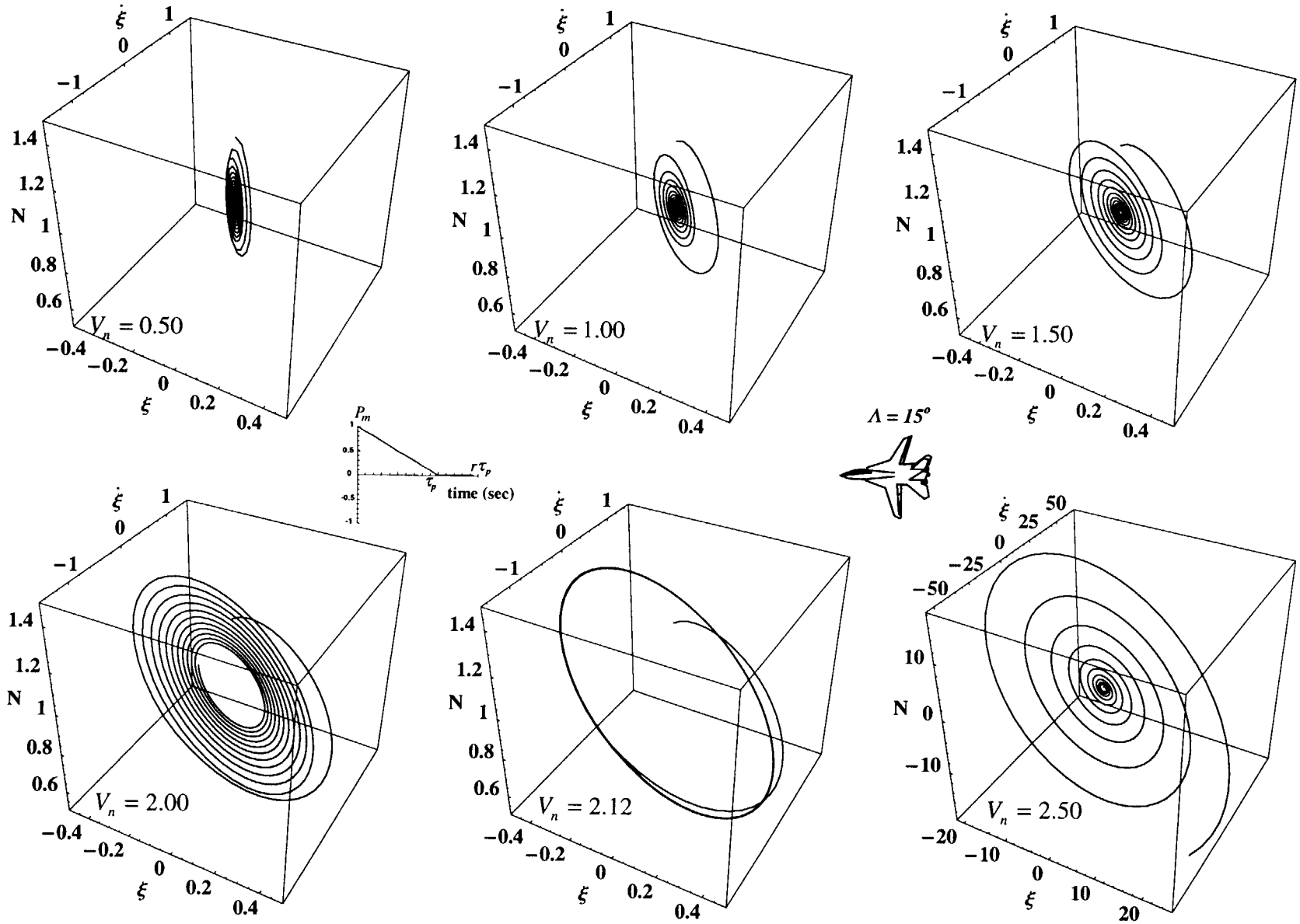

Fig. 12

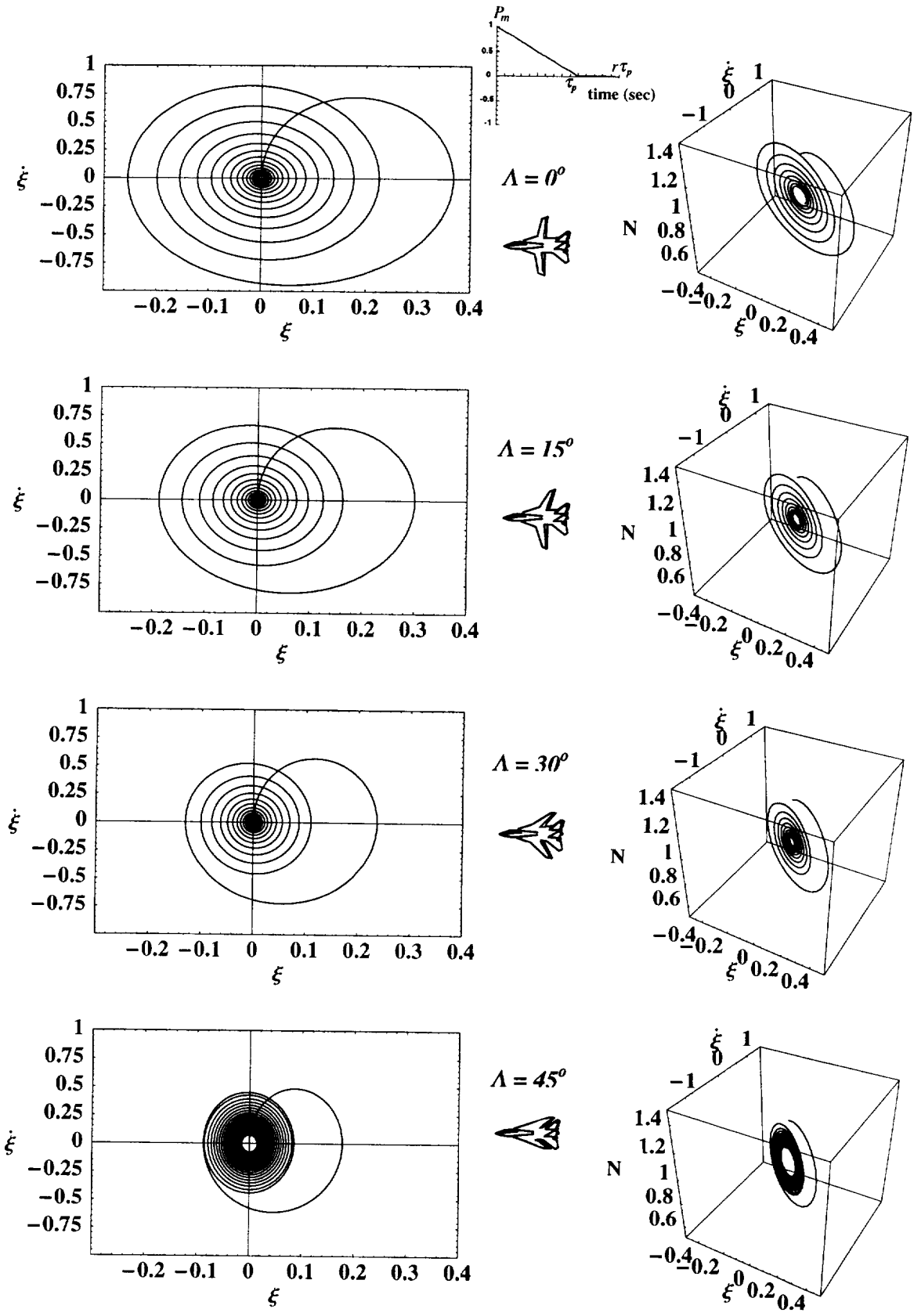
P_m
$r\tau_p$
τ_p
time (sec)
$\Lambda = 0^o$
$\Lambda = 15^o$
$\Lambda = 30^o$
$\Lambda = 45^o$
$\dot{\xi}$
ξ
N

Fig. 13

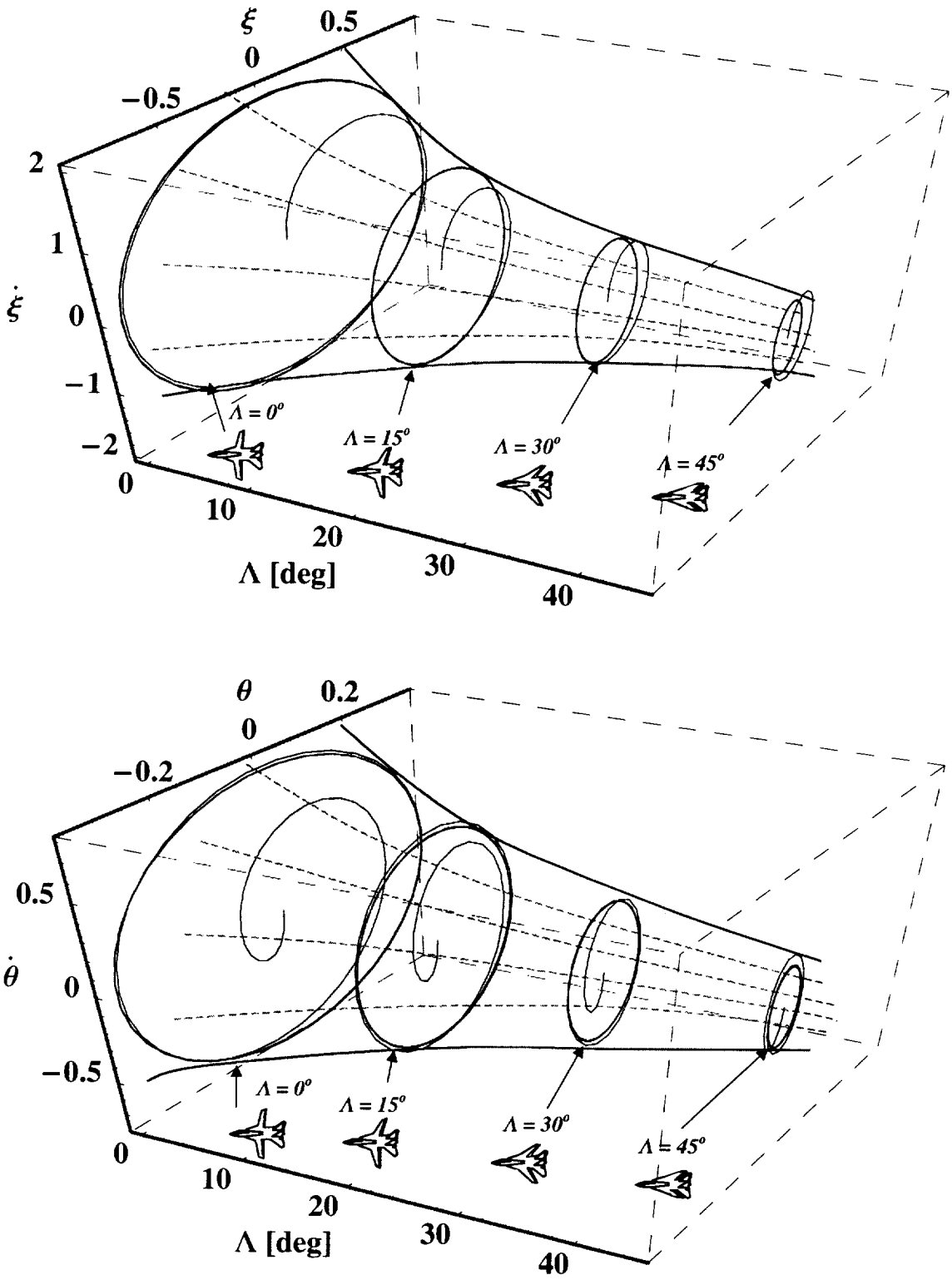
ξ
0.5
0
−0.5
2
1
0
−1
−2
ξ̇
0
10
20
30
40
Λ [deg]
Λ = 0°
Λ = 15°
Λ = 30°
Λ = 45°
θ
0.2
0
−0.2
0.5
0
−0.5
θ̇
0
10
20
30
40
Λ [deg]
Λ = 0°
Λ = 15°
Λ = 30°
Λ = 45°

Fig. 14